

High-Order Methods for the Numerical Simulation of Vortical and Turbulent Flows

Spectral methods for compressible reactive flows

David Gottlieb^{a,1,*}, Sigal Gottlieb^{b,2}

^a *Division of Applied Mathematics, Brown University, Providence, RI, USA*

^b *University of Massachusetts Dartmouth, North Dartmouth, MA, USA*

Available online 28 December 2004

Abstract

High order simulations are necessary in order to capture fine details in resolving supersonic reactive flows. However, high Mach number compressible flows feature sharp gradients and discontinuities, which present a challenge to successful simulations using high order methods. Spectral methods have proven a powerful tool in simulation of incompressible turbulent flows, and recent advances allow the application of spectral methods to compressible reactive flows. We review the recent advances in the theory and application of spectral methods which allow stable computations of discontinuous phenomena, and the recovery of high order information via postprocessing, and present applications of high Mach number reactive flows. **To cite this article:** *D. Gottlieb, S. Gottlieb, C. R. Mecanique 333 (2005).*

© 2004 Académie des sciences. Published by Elsevier SAS. All rights reserved.

Keywords: Computational fluid mechanics; Reactive flows; Spectral methods; Gegenbauer postprocessing; Shock-waves; Richtmyer–Meshkov

1. Introduction

High order methods are the choice methods in numerical computations requiring fine scale resolution and long time integrations. In particular, spectral methods have contributed to our understanding of turbulence by successfully simulating incompressible turbulent flows. Several issues arise when applying spectral methods to high Mach number compressible flows, which feature sharp gradients and discontinuities. In the presence of such phenomena the accuracy of high order methods deteriorates. This is due to the well known Gibbs phenomenon that states that the pointwise convergence of global approximations of discontinuous functions is at most first order. In this case the approximations are oscillatory and converge nonuniformly, seemingly rendering global methods, such as spectral methods, useless for simulating compressible flows.

* Corresponding author.

¹ This work was supported by AFOSR grant F49620-02-1-0113 and DOE grant DE-FG02-98ER25346.

² This work was supported by NSF grant no. DMS 0106743.

Recent advances in the theory and application of spectral methods indicate that high order information is retained in stable spectral simulations of discontinuous phenomena and can be recovered by suitable postprocessing techniques. The goal of this paper is to review the state of the art in applying spectral methods to the numerical solution of discontinuous problems.

In Section 2 we briefly review the issues involved in global approximations of nonsmooth functions. We present sufficient conditions under which high order information may be extracted by postprocessing, and discuss some recently developed postprocessors. The question is whether spectral approximations of discontinuous solutions of partial differential equations retain high order accurate information. We review the theory for linear hyperbolic equations in Section 3 and explain why and how high order accuracy information is retained in high order simulations of linear discontinuous problems. In Section 4 we discuss the stabilization of spectral methods applied to nonlinear hyperbolic equations and in Section 5 we present efficient ways of stabilizing these schemes using adaptive filters. In Section 6 we bring numerical evidence that design accuracy can be achieved even for nonlinear systems of equations after postprocessing. Several examples of successful applications of spectral methods to complicated interactions of shock waves and complex flows are presented in Section 7. Many more contributions have been made in [1–19].

2. Approximation theory

The partial Fourier sum

$$\sum_{k=-N}^N \hat{f}_k e^{\pi i k x}$$

based on the first $2N + 1$ Fourier coefficients of a nonsmooth function $f(x)$, converges slowly away from the discontinuity and features non-decaying oscillations. This behavior of global approximations of nonsmooth functions is known as the classical Gibbs phenomenon. (See [20].) The same behavior is observed for all global approximations such as orthogonal polynomials, Bessel functions, etc.

In this section we present sufficient conditions for the removal of the Gibbs phenomenon and show that these conditions are satisfied for all commonly used spectral approximations (Fourier, Chebyshev and Legendre). The main result can be summarized as follows: the slow convergence of the expansion of a discontinuous function in any basis can be completely overcome, in any interval of smoothness, provided that this basis has a Gibbs complementary basis (to be defined later).

Consider a function $f(x) \in L^2[-1, 1]$ and assume that there is a subinterval $[a, b] \subset [-1, 1]$ in which $f(x)$ is analytic. Let the family $\{\Psi_k(x)\}$, be orthonormal under a scalar product (\cdot, \cdot) , and denote the finite expansion of $f(x)$ in this basis by $f_N(x)$,

$$f_N(x) = \sum_{k=0}^N (f, \Psi_k) \Psi_k(x)$$

The standard assumption is

$$\lim_{N \rightarrow \infty} |f(x) - f_N(x)| = 0$$

almost everywhere in $x \in [-1, 1]$. This assumption is satisfied by all commonly used spectral methods. However, this convergence is pointwise and nonuniform, and the rate of convergence is low. For convenience we define the local variable, $\xi = -1 + 2\frac{x-a}{b-a}$ such that if $a \leq x \leq b$ then $-1 \leq \xi \leq 1$.

Definition 2.1 (*Gibbs Complementary Basis*). The two parameter family $\{\Phi_k^\lambda(\xi)\}$ is Gibbs complementary to the family $\{\Psi_k(x)\}$ if the following are satisfied:

(a) *Orthogonality*

$$\langle \Phi_k^\lambda(\xi), \Phi_l^\lambda(\xi) \rangle_\lambda = \delta_{kl}$$

For some local inner product $\langle \cdot, \cdot \rangle_\lambda$. Note that the scalar product $\langle \cdot, \cdot \rangle_\lambda$ is defined only in the interval $[a, b]$ and may be very different from the scalar product (\cdot, \cdot) which is defined on the interval $[-1, 1]$ e.g. as defined in (1).

(b) *Spectral Convergence*

The expansion of an analytic function $g(\xi)$ in the basis $\Phi_k^\lambda(\xi)$ converges exponentially fast, i.e.

$$\max_{-1 \leq \xi \leq 1} \left| g(\xi) - \sum_{k=0}^{\lambda} \langle g, \Phi_k^\lambda \rangle_\lambda \Phi_k^\lambda(\xi) \right| \leq e^{-q_1 \lambda}, \quad q_1 > 0$$

(c) *The Gibbs Condition*

There exists a number $\beta < 1$ such that if $\lambda = \beta N$ then

$$\left| \langle \Phi_l^\lambda(\xi), \Psi_k(x(\xi)) \rangle_\lambda \right| \max_{-1 \leq \xi \leq 1} |\Phi_l^\lambda(\xi)| \leq \left(\frac{\alpha N}{k} \right)^\lambda, \quad k > N, l \leq \lambda, \alpha < 1$$

Condition (b) implies that the expansion of a function g in the basis $\{\Phi_l^\lambda(\xi)\}$ converges exponentially fast if g is analytic in $-1 \leq \xi \leq 1$ (corresponding to $a \leq x \leq b$). Condition (c) states that the projection of $\{\Psi_k\}$ for large k on the low modes in $\Phi_l^\lambda(\xi)$ with small l is exponentially small in the interval $-1 \leq \xi \leq 1$.

The main result is now stated as a theorem [21].

Theorem 2.2 (The General Gibbs Resolution Theorem). *Let $f(x) \in L^2[-1, 1]$ and analytic in $[a, b] \subset [-1, 1]$. $\{\Psi_k(x)\}$ is an orthonormal family with the inner product (\cdot, \cdot) . The family $\{\Phi_k^\lambda(\xi)\}$ is Gibbs complementary to the family $\{\Psi_k(x)\}$ as defined in (a)–(c), with $\lambda = \beta N$.*

Then

$$\max_{a \leq x \leq b} \left| f(x) - \sum_{l=0}^{\lambda} \langle f_N, \Phi_l^\lambda \rangle_\lambda \Phi_l^\lambda(\xi(x)) \right| \leq e^{-qN}, \quad q > 0$$

The theorem states that if we are given the expansion coefficients (f, Ψ_k) of a discontinuous function, then even if the series

$$\sum_{k=0}^N (f, \Psi_k) \Psi_k(x)$$

converges slowly it is still possible to get a rapidly converging approximation to $f(x)$, in any interval free of discontinuity, if one can find another a family that is Gibbs complementary to the original basis. In practice this can be accomplished when intervals of smoothness are known.

In a series of papers we showed that the Gegenbauer polynomials

$$\Phi_k^\lambda(\xi) = \frac{1}{\sqrt{h_k^\lambda}} C_k^\lambda(\xi)$$

which are orthonormal under the inner product $\langle \cdot, \cdot \rangle_\lambda$ defined by

$$\langle f, g \rangle_\lambda = \int_{-1}^1 (1 - \xi^2)^{\lambda-1/2} f(\xi) g(\xi) d\xi \tag{1}$$

are Gibbs complementary to all commonly used spectral approximations:

Theorem 2.3. Let $\beta = \frac{2\pi\epsilon}{27}$. Then the Gegenbauer polynomials satisfy the condition:

$$\left| \int_{-1}^1 (1 - \xi^2)^{\lambda-1/2} C_l^\lambda(\xi) \Psi_k(x(\xi)) d\xi \right| \leq \left(\frac{\alpha N}{k} \right)^\lambda$$

for $k > N$, $l \leq \lambda = \beta N$, $0 < \alpha < 1$. For $\Psi_k(x) = \frac{1}{2} e^{ik\pi x}$, $|k| \leq \infty$ (Fourier Functions); For $\Psi_k(x) = (1/\sqrt{h_k^{1/2}}) C_k^0(x)$ (Chebyshev polynomials) and for $\Psi_k(x) = (1/\sqrt{h_k^\mu}) C_k^\mu(x)$ (Gegenbauer polynomials, note that $\mu = \frac{1}{2}$ corresponds to the Legendre polynomials).

2.1. The inverse Gegenbauer method

The theory presented in [20] does not prescribe an optimal way of constructing a Gibbs complementary basis. The Gegenbauer method is not robust, it is sensitive to roundoff errors and to the choice of the parameters λ and m . A different implementation of the Gegenbauer postprocessing method has been suggested recently by Shizgal and Jung [22]. To explain the differences between the direct Gegenbauer method and the inverse Gegenbauer method suggested in [22], consider the case of the Fourier expansion of a nonperiodic problem. The Fourier approximation $f_N(x)$ of $f(x)$

$$f_N(x) = \sum_{k=-N}^N \hat{f}_k e^{ik\pi x}$$

where $\hat{f}_k = (f(x), e^{ik\pi x})$, and we construct

$$f_N^m(x) = \sum_{l=0}^m \hat{g}_l C_l^\lambda(x)$$

where $\hat{g}_l = (f_N, C_l^\lambda(x))_\lambda$. In the Inverse method we use the relationship

$$\hat{f}_k = (f_N^m(x), e^{ik\pi x})$$

and invert to find \hat{g}_l .

Thus if we define the matrix $W_{kl} = (C_l^\lambda(x), e^{ik\pi x}) = \frac{1}{2} \int_{-1}^1 C_l^\lambda(x) e^{ik\pi x} dx$, and $\hat{f}_k = (f, e^{ik\pi x})$

$$\sum_{l=0}^m W_{kl} g_l^\lambda = \hat{f}_k$$

The method seems to be less sensitive to roundoff errors or to the choice of parameters. In particular if the original function is a polynomial, the inverse method is exact. The authors proved that the Inverse method converges exponentially for any λ demonstrating great improvement over the direct method. On the other hand for $m > 20$ the matrices are ill conditioned.

2.2. Fourier–Padé approximations

The methods discussed in the previous sections require the knowledge of the position of discontinuity. In the Padé approximation no such knowledge is necessarily required.

Padé rational approximations have been considered as postprocessors for polynomials by several authors [23–25]. Padé reconstruction recovers a non-oscillatory solution with a reduced overshoot at the singularity. This is due to the possible existence of poles of some order for the denominator of Padé approximant. Geer and his coworkers [25], suggested a nonlinear way of implementing the rational trigonometric approximations for even or odd 2π -periodic piecewise smooth functions. In [24], the Fourier expansion is treated as a Laurent expansion, and using the Fourier–Padé rational approach, the spectral convergence is obtained up to the discontinuity by subtracting off the jump from the Fourier data, which requires the advance knowledge not only of position the singularity, but also the magnitude of the jump. In our recent [26] work, we have designed two Fourier–Padé methods considering the general case of piecewise analytic functions with no advance knowledge of the singularity. Simple ways of implementing Fourier–Padé Galerkin and Fourier–Padé collocation methods have been developed and applied to simulate the solutions of nonlinear partial differential equations. Currently we study the merits of these methods when applied to PDEs.

3. Linear hyperbolic equations

In the last section we demonstrated that spectral accuracy can be recovered in spectral approximations of non-smooth functions. In this section we will review the same result for discontinuous solutions of linear hyperbolic equations.

Consider the hyperbolic system of the form

$$\frac{\partial U}{\partial t} = \mathcal{L}U$$

with initial conditions

$$U(t = 0) = U_0$$

The linearized Euler equations of gas dynamics is an example of such a system.

Let u be the Fourier Galerkin approximation given by:

$$\begin{aligned} \left(\frac{\partial u}{\partial t} - \mathcal{L}u, e^{i\pi kx} \right) &= 0, \quad -N \leq k \leq N \\ (U_0 - u_0, e^{i\pi kx}) &= 0, \quad -N \leq k \leq N \end{aligned}$$

For smooth solutions we have the classical error estimate:

$$\|U - u\| \leq K \|U_0\|_s \frac{1}{N^{s-1}}$$

This estimate, obviously, requires the initial condition to be smooth everywhere and does not apply in the case of piecewise smooth initial conditions. However, it has been proven in [27] that:

$$|(U(T) - u(T), \phi)| \leq K \|\phi\|_s \frac{1}{N^s} \quad (2)$$

for any smooth function ϕ . Similar results are obtained for the collocation (pseudospectral) method. However, the numerical initial condition (u_0) has to be the Galerkin approximation to the initial condition U_0 . Alternatively, a suitably preprocessed numerical initial condition should be used. The same results hold for Legendre and Chebyshev methods.

Eq. (2) implies that the Fourier coefficients of u approximate those of U with spectral accuracy. It is therefore possible to postprocess to get spectral accuracy for the point values in any interval where the solution U is smooth.

4. Nonlinear equations

The arguments presented in Section 3, demonstrating the possibility of extracting high order information from spectral methods applied to linear equations, do not hold in the nonlinear case. However, Lax [28] argued that high order information is contained in a convergent high resolution scheme. Several important advances have been made towards establishing the convergence of spectral approximations when applied to nonlinear hyperbolic equations.

Consider the nonlinear hyperbolic system

$$\frac{\partial U}{\partial t} + \frac{\partial f(U)}{\partial x} = 0 \quad (3)$$

The Fourier Galerkin method can be written as

$$\frac{\partial u_N}{\partial t} + \frac{\partial \mathcal{P}_N f(u_N)}{\partial x} = 0 \quad (4)$$

The method is unstable in general but can be stabilized by either the following methods:

- In the *Spectral Viscosity Method (SV)* (see [29–31]) (4) is modified:

$$\frac{\partial u_N}{\partial t} + \frac{\partial \mathcal{P}_N f(u_N)}{\partial x} = \epsilon_N (-1)^{s+1} \frac{\partial^s}{\partial x^s} \left[Q_m(x, t) * \frac{\partial^s u_N}{\partial x^s} \right]$$

where the operator Q_m keeps only the high modes of the viscosity term $\frac{\partial^2}{\partial x^2} u_n$:

$$\epsilon_N (-1)^{s+1} \frac{\partial^s}{\partial x^s} \left[Q_m(x, t) * \frac{\partial^s u_N}{\partial x^s} \right] \sim \epsilon \sum_{m < |k| < N} (ik)^{2s} \widehat{Q}_k \widehat{u}_k e^{ikx}$$

with

$$\epsilon \sim CN^{2s-1}; \quad m \sim N^\theta, \quad \theta < \frac{2s-1}{2s}; \quad 1 - \left(\frac{m}{|k|} \right)^{(2s-1)/\theta} \leq \widehat{Q}_k \leq 1$$

- A better way to stabilize the scheme is the *Super Spectral Viscosity (SSV)* method.

$$\frac{\partial u_N}{\partial t} + \frac{\partial \mathcal{P}_N f(u_N)}{\partial x} = \epsilon_N (-1)^{s+1} \frac{\partial^{2s}}{\partial x^{2s}} u_N \quad (5)$$

The stabilization techniques apply also to the Fourier collocation operator I_N . For the polynomial methods the SSV viscosity term on the right-hand side of (5) is modified as follows: $(-1)^{s-1} (\sqrt{1-x^2} \frac{\partial}{\partial x})^{2s}$ and $(-1)^{s-1} (\frac{\partial}{\partial x} (1-x^2) \frac{\partial}{\partial x})^s$ for the Chebyshev and Legendre methods respectively.

Note that for spectral accuracy the order s must be proportional to N , the number of polynomials (or grid points) in the approximation. Thus viscosity changes with mesh refinement.

The theory developed by Tadmor and Tadmor and Maday (see [29–32]) demonstrates that both the SV and SSV methods converge to the correct entropy solution for Fourier and Legendre approximations to scalar nonlinear hyperbolic equations. Carpenter, Gottlieb and Shu [33] proved that even for systems, if the solution converges it converges to the correct entropy solution.

5. Adaptive filtering

The straightforward use of the SV and SSV methods requires extra derivative computations thus effectively doubling the computational cost. For this reason, most of the large scale spectral codes for high Mach number

flows use filtering to stabilize the code. In fact, as will be explained in this section, filtering can be seen as an efficient way of applying the SV and SSV methods.

To understand the relationship between the superviscosity method and the filtering method let

$$u_N(x, t) = \sum_{k=0}^N a_k(t) \phi_k(x)$$

where ϕ_k are the basis function used (Fourier, Chebyshev or Legendre). Also, let $b_k(a_0, \dots, a_N)$ be the coefficients in the expansion

$$P_N f(u_N) = \sum_{k=0}^N b_k(t) \phi_k(x)$$

Then (5) can be written as

$$\frac{\partial a_k}{\partial t} = b_k - c \epsilon_N k^{2s} a_k \quad (6)$$

Thus a typical step in a Runge–Kutta method for the SSV method can be written as:

$$a_k^{n+1} = a_k^n + \Delta t b_k^n - \Delta t c \epsilon_N k^{2s} a_k^{n+1}$$

Note that the stabilizing term is implicit, to prevent further limitation on the time step. In the filtering method we change slightly the last term

$$a_k^{n+1} = a_k^n + \Delta t b_k^n + (1 - e^{\Delta t c \epsilon_N k^{2s}}) a_k^{n+1}$$

yielding

$$a_k^{n+1} = e^{-\Delta t c \epsilon_N k^{2s}} (a_k^n + \Delta t b_k^n)$$

This is an exponential filter. The benefit of this method is that it does not require any extra derivative computation and therefore does not increase the computational cost.

We note here that the parameter s can be a function of the spatial station x . This means that in different regions one can use viscosity terms of different orders. In the presence of local sharp gradients one should reduce the order of the filter. To keep the spectral accuracy, though, s should be an increasing function of N .

Thus the local adaptive filter is defined by

$$u_N^\sigma = \sum_{k=0}^N \sigma\left(\frac{k}{N}\right) a_k(t) \phi_k(x) \quad (7)$$

where

$$\sigma(\omega) = e^{-\alpha \omega^{2\gamma s}} \quad (8)$$

As mentioned $\gamma = \gamma(x)$ can change within the domain.

6. Numerical evidence for high order accuracy

In this section we will present two examples which demonstrate that (formal) high order methods yield, indeed, high order information that can be extracted by appropriate post processing. The first example involves the Fourier method solution of the scalar Burgers equation

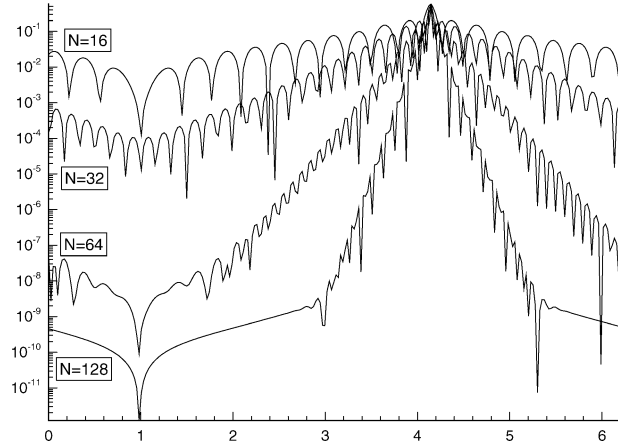


Fig. 1. Spectral accuracy for the Burgers equation.

$$U_t + \left(\frac{1}{2} U^2 \right)_x = 0, \quad x \in [0, 2\pi), \quad U(x, 0) = \sin(x)$$

with periodic boundary conditions. In time a shock develops and moves around the domain. The unpostprocessed solution is first order accurate. However, Shu and Wang [34] recovered spectral accuracy, everywhere in the domain, after post processing. Fig. 1 depicts the point errors in the postprocessed solution of the Burgers equation. The rate of decrease of the error improves with the number of points, indicating spectral accuracy.

The second example [35] involves the WENO code for the quasi-one-dimensional nozzle flow. The governing equations are the usual Euler system plus a source term:

$$\begin{pmatrix} \rho \\ \rho u \\ E \end{pmatrix}_t + \begin{pmatrix} \rho u \\ P + \rho u^2 \\ u(P + E) \end{pmatrix}_x = -\frac{A_x}{A} \begin{pmatrix} \rho u \\ \rho u^2 \\ u(P + E) \end{pmatrix}$$

where ρ , u , P , and E are the density, velocity, pressure and total specific energy (respectively), and $A = A(x)$ is the cross area function of the nozzle and $A_x = \frac{dA}{dx}$. The shape of the nozzle is calculated by the requirement of linear distribution of Mach number from $M = 0.8$ at the inlet to $M = 1.8$ at the exit assuming the flow is isentropic and fully expanded. The equation of state is

$$P = (\gamma - 1)\rho \left(E - \frac{1}{2}u^2 \right)$$

We compute the solution at steady-state by marching in time until the residuals go down to machine zero. The steady-state solution has a shock halfway across the domain. We separate the domain into two regions in space, the left of the shock and the right of the shock. In each of these regions the solution is analytic. The region to the right of the shock contains information that traveled through the shock, the left does not. As expected, the region to the left maintains high order accuracy away from the shock, while in the region to the right of the shock, the error is only first order accurate (Table 1). After postprocessing the region to the right of the shock, high order accuracy is recovered (Table 2). In the calculation of the error we exclude the point of the shock and one additional point. Thus, the domain in which we are measuring the error is actually getting closer and closer to the shock as N increases (demonstrating uniform convergence). The infinity norm error is thus $O(1)$ before postprocessing (which is in agreement with the behavior of the Gibbs phenomenon right near the discontinuity) but the order increases dramatically after postprocessing.

Table 1

The errors from the steady state computation (Example 1), before postprocessing. The errors are calculated up to one gridpoint away from the shock

n	l_2 error	order	l_∞ error
600	0.0000986		0.00137
800	0.0000699	1.19	0.00109
1000	0.0000655	0.29	0.00127
1200	0.0000584	0.63	0.00119
1400	0.0000554	0.34	0.00127
1600	0.0000508	0.65	0.00119
1800	0.0000479	0.50	0.00119

Table 2

The errors from the steady state computation (Example 1), after postprocessing. The errors are calculated up to one gridpoint away from the shock

n	λ	m	l_2 error	l_2 order	l_∞ error	l_∞ order
600	3	3	0.00016065		0.000816	
800	3	4	0.00005823	3.52	0.000333	3.11
1000	4	5	0.00002605	3.6	0.000166	3.13
1200	5	6	0.00001313	3.75	0.0000819	3.8
1400	6	7	0.000006169	4.9	0.0000409	4.5
1600	6	8	0.000003968	3.30	0.00001726	6.46
1800	7	9	0.000002528	3.83	0.000008953	5.57

7. Computational results

There is extensive literature reporting results of the application of spectral methods to shock wave problems (see for example [36,37,29,30,32,31]). In this section we do not attempt to review this literature. We will rather discuss here some selective cases of applications of spectral methods to complicated interactions of shock waves and complex flow patterns. For those problems, high order accuracy is vitally needed to capture fine details of the flow. In [38], the author considered interactions of shock waves and entropy waves as well as interactions of shock waves and vortices. The calculations involved solutions of the two dimensional Euler equations and the results compared well with ENO methods.

In [39] the authors compared ENO and spectral methods for the numerical simulations of shock–cylinder interactions in the case of reactive flows. The authors demonstrated that spectral methods required less resources than the ENO schemes for comparable accuracy.

A more extensive study of spectral simulations of compressible reactive high Mach number flows has been reported in [40]. In this work the interaction of shock waves and hydrogen jets were studied. This involve the solution of the Navier–Stokes equations with chemical interactions. The work gives a clear demonstration of the fact that spectral methods are very suitable for studies of complicated flows that involve shock waves. The mixing and fuel breaking were obtained very accurately. A series of numerical simulations are carried out to investigate the convergence properties of both the Spectral scheme and the WENO scheme. The spectral calculations display the fine structural details of the mixing inside the hydrogen jet, and patterns of combustion. In Fig. 2 we present the flow field resulting from interactions of shock waves and hydrogen jets.

We would like here to present some yet unpublished results concerning the Richtmyer–Meshkov instabilities. The Richtmyer–Meshkov Instability (RMI) can be defined in its simplest form as the resulting flow when a shock impinges on the interface between two materials, fluids, etc. When the interface between the substances is not parallel to the shock front, vorticity will be induced. The RMI is encountered in a variety of physical contexts such as in the mixing of fuel with oxidants in SCRAMjets and in Inertial Confinement Fusion (ICF). From the point of view of the numerical calculation, we can break the RMI problem into two parts. First, we have the issue of reliably calculating the motion of a possibly very strong shock wave, and second, we have the issue of reliably calculating the mix that ensues after this shock wave accelerates the interface. It is in this second area of calculating the ensuing mix where high order numerical schemes offer unparalleled efficiency. In the following we bring comparisons of two high order schemes, the WENO scheme and spectral methods. Simulations, using various interface thicknesses and resolutions, are computed and terminated at some representative time after the shock had transmitted sufficiently far away from the interface and before exiting the physical domain.

As evidenced from the results of the Spectral and the WENO calculations shown below, the following major features of the Richtmyer–Meshkov instability can be observed (see Fig. 3) at time $t = 50 \times 10^{-6}$ s, namely,

- Wave generated by the shock refraction behind the gas interface in Box 1.

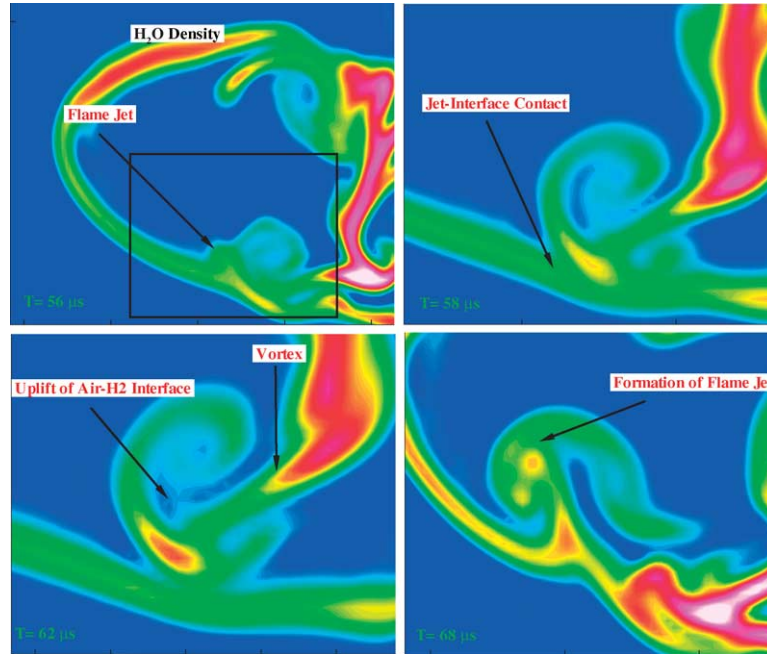


Fig. 2. Flame production as a result of shock hydrogen jet interaction.

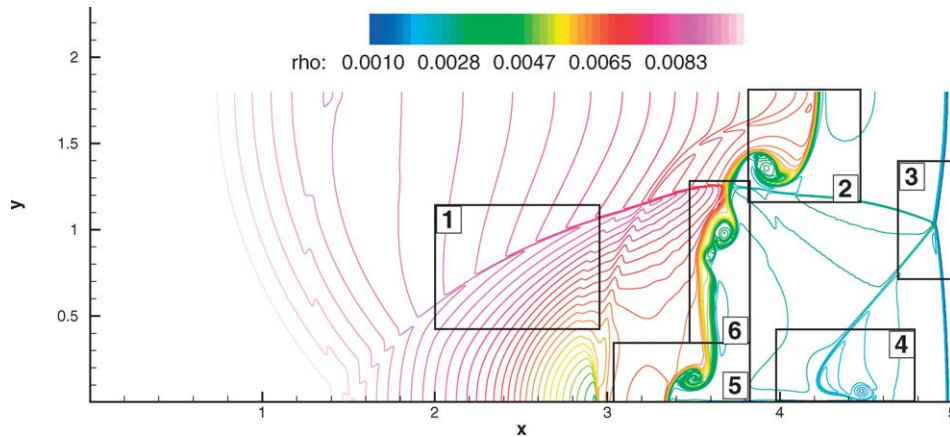


Fig. 3. The numbered regions enclose the most prominent flow features of the Richtmyer–Meshkov instability at time $t = 50 \times 10^{-6}$ s.

- The penetration of the heavy (Xe) to light (Ar) fluid causes the deformation of the interface into a large mushroom shape structures in Box 2 and the opposite in Box 5. They are referred as Spike and Bubble respectively, in the literatures. They move in the opposite direction relative to each other and form a ever larger turbulence mixing zone.
- Pressure wave along the transmitted shock in Box 3.
- A small jet and its vortical structure located in Box 4. The contact discontinuity develops into a more complicated vortical rollups in a finer and long term simulation, possibly caused by the Kelvin–Helmholtz instability.
- Vortical rollups of the gaseous interface inside Box 6.

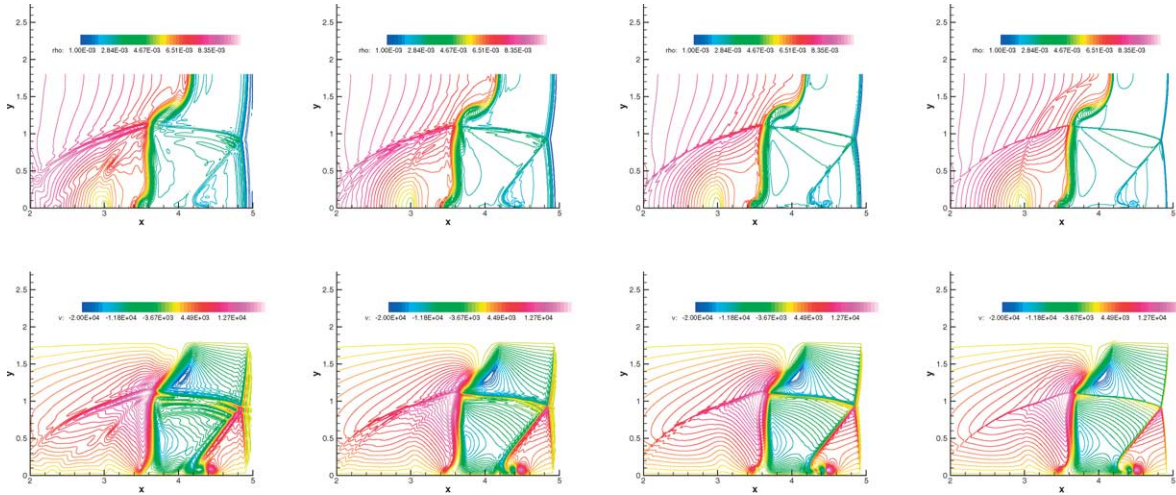


Fig. 4. Convergence Study $\delta = 0.6$ cm: density (top row) and V-velocity (bottom row) contour plot of the Richtmyer–Meshkov instability as computed by the Spectral scheme and the WENO-LF-5 scheme. Domain length in x is $L_x = 5$ cm. The interface thickness $\delta = 0.6$ cm. The final time is $t = 50 \times 10^{-6}$ s. The resolution of the Spectral schemes are 256×128 (left), 512×256 (middle left) and 1024×512 (middle right) and the WENO scheme is 1024×512 (right).

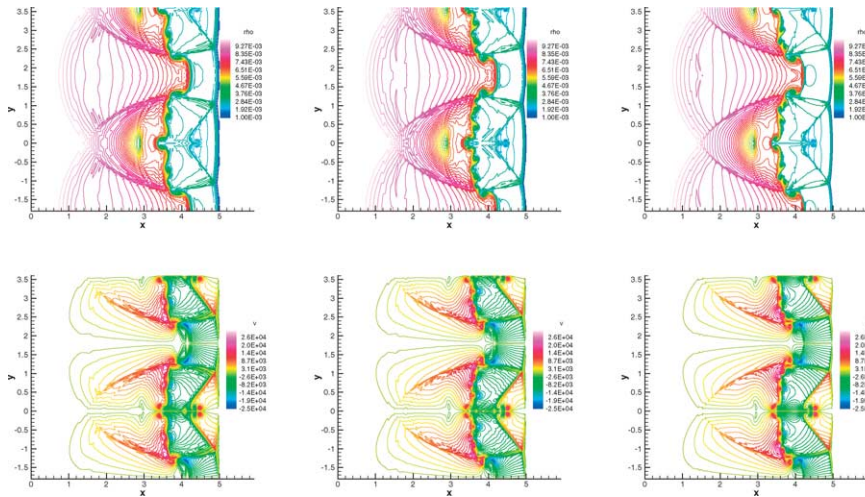


Fig. 5. Convergence study $\delta = 0.2$ cm: density (top row) and V-velocity (bottom row) contour plot of the Richtmyer–Meshkov instability as computed by the Spectral scheme. Domain length in x is $L_x = 5$ cm. The interface thickness $\delta = 0.2$ cm. The final time is $t = 50 \times 10^{-6}$ s. The resolution of the spectral schemes are 384×192 (left), 512×256 (middle) and 1024×256 (right).

The global large and median features (Box 1, 2, 3, 4 and 5) are well captured accurately by both numerical schemes for a given resolution. It is unclear, however, if the smaller rollups along the gases interface (Box 6) presented in the high resolution/high order cases are physical due to the non-dissipative nature of the Euler equations or numerical due to the oscillatory nature of the numerical schemes or both.

For long time integration, the smoothest of the gaseous interface at the earlier development yields a slightly smoother and rounder interface shape at the later time as seen in the WENO calculation. The overall global structures, however, seem to agree very well among the calculations performed here.

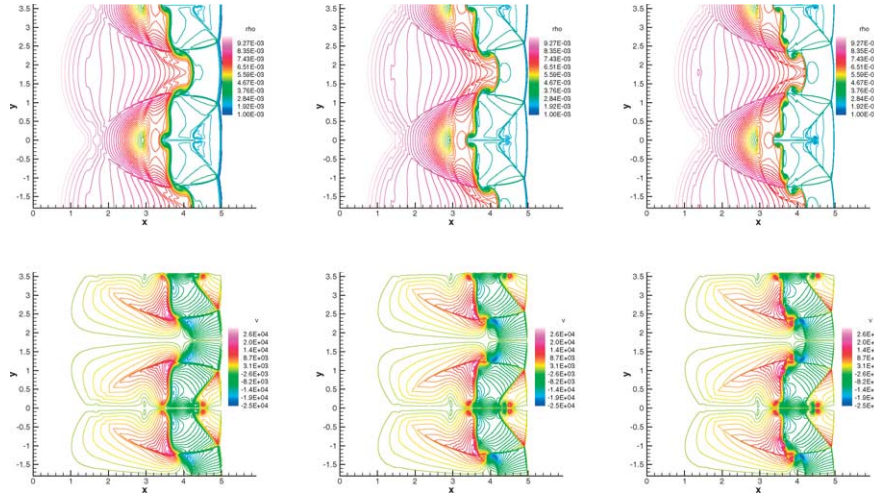


Fig. 6. Convergence study $\delta = 0.2$ cm: density (top row) and V-velocity (bottom row) contour plot of the Richtmyer–Meshkov instability as computed by the WENO-LF-5 scheme. Domain length in x is $L_x = 5$ cm. The interface thickness $\delta = 0.2$ cm. The final time is $t = 50 \times 10^{-6}$ s. The resolution of the WENO-LF-5 schemes are 256×128 (left), 512×256 (middle) and 1024×512 (right).

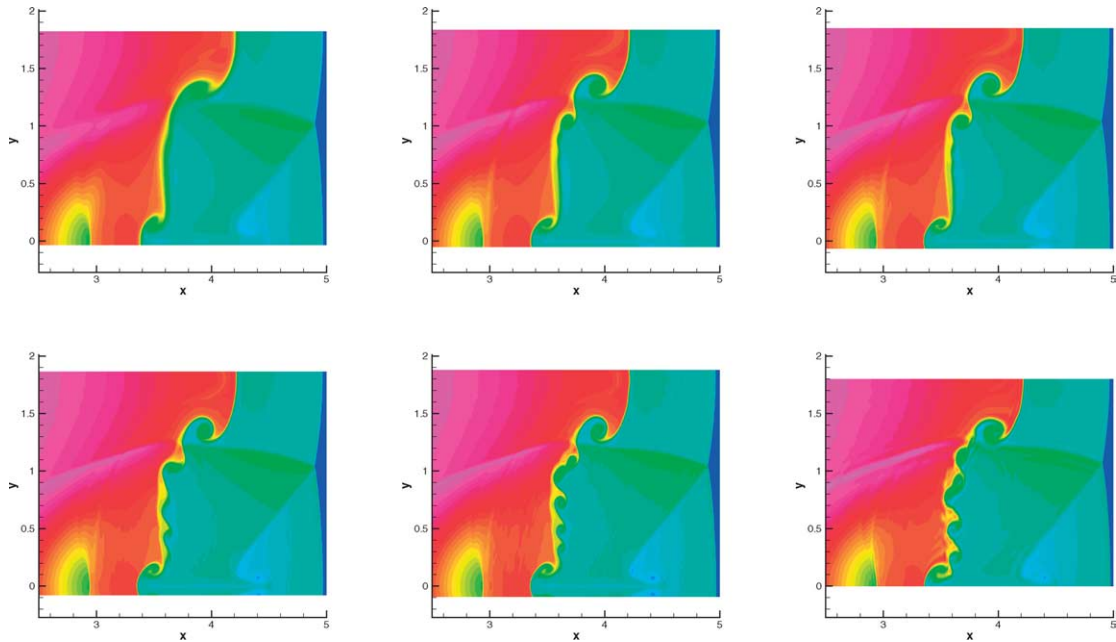


Fig. 7. Comparisons of WENO of different orders and Spectral methods. Third order WENO on top left, fifth order on top middle, seventh order – top right, ninth order – bottom left, eleventh order – bottom middle and spectral on bottom right.

We first examine the convergence properties of both the Spectral scheme and the WENO-LF-5 finite difference scheme. For this, we used a thicker interface with $\delta = 0.6$ cm to establish the convergence of the numerical schemes of the large and medium scale structures (Fig. 4). This avoids the possible contamination of numerical artifacts due to high gradients generated along the shock-interface interaction and bypass the issue of under-resolved fine scale physical structures. Furthermore, the spectral solutions are not post-processed by any existing post-processing

algorithms to remove the Gibbs oscillations. It can be observed that the large and medium scale structures such as the transmitted shock, the location of the triple point, the shocked-interface velocity, pressure waves and vorticity generation, are basically in excellent agreement with each others. The weak vertical wave located downstream behind the interface is a left over entropy wave from the initial shock condition.

Next we examine the case in which the interface thickness is reduced from $\delta = 0.6$ cm to $\delta = 0.2$ cm. The density ρ and velocity V of the solution of the Spectral and WENO-LF-5 runs are shown in Figs. 5 and 6 respectively, at time $t = 50 \times 10^{-6}$ s with various resolutions. Here too it can be observed that the large and median scale structures such as transmitted shock, shocked-interface velocity and shock triple point are in excellent agreement with each others. Some discrepancies of the fine scale structures along the gaseous interface, as can be expected for numerical simulations of solutions which are sensitive to perturbation in nature, are observed.

In Fig. 7 we compare the structure of the interface as computed by WENO schemes of different orders (third to eleventh), and spectral methods. It is clear that the WENO results converge to the spectral ones as the order of accuracy is raised.

It is evident from the extensive numerical studies that spectral methods can serve as a useful tool in simulating flows exhibiting unsteady fine structures. In particular spectral methods proved to accurately capture the details of high Mach number compressible reactive flows.

Acknowledgements

The authors wish to thank Professor W.S. Don who provided the numerical results in Section 7.

References

- [1] A.N. Aleshin, E.I. Chebotareva, V.V. Krivets, E.V. Lazareva, S.V. Sergeev, S.N. Titov, S.G. Zaytsev, Investigation of evolution of interface after its interaction with shock waves, Report No. 06-96, LANL.
- [2] H. Cabannes, Padé approximants method and its applications to mechanics, in: J. Ehlers, K. Hepp, H.A. Weidenmüller, J. Zittartz (Eds.), in: *Lecture Notes in Phys.*, Springer-Verlag, New York, 1976.
- [3] W.S. Don, B. Costa, PseudoPack 2000: Numerical Library for Pseudospectral Differentiation.
- [4] W.S. Don, D. Gottlieb, High order methods for complicated flows interacting with shock waves, AIAA 97-0538.
- [5] W.S. Don, D. Gottlieb, J.H. Jung, A multi-domain spectral method for supersonic reactive flows, *J. Comput. Phys.*, submitted for publication.
- [6] W.S. Don, D. Gottlieb, J.H. Jung, Multi-domain spectral method approach to supersonic combustion of recessed cavity flame-holders, JANNAF 38th Combustion, 26th Airbreathing Propulsion, 20th Propulsion Systems Hazards, and 2nd Modeling and Simulation Subcommittees Joint Meeting, held in Destin, FL 8–12 April 2002.
- [7] W.S. Don, D. Gottlieb, C.W. Shu, High order numerical methods for the two dimensional Richtmyer–Meshkov Instability, Part I, in: *Conference Proceeding for the International Workshop for the Physics of Compressible Turbulence Mixing, Laser and Particle Beams*, in press.
- [8] D. Gottlieb, S.A. Orszag, *Numerical Analysis of Spectral Methods: Theory and Applications*, CBMS Conf. Ser. in Appl. Math., vol. 26, SIAM, 1977.
- [9] D. Gottlieb, M.Y. Hussaini, S.A. Orszag, Introduction: theory and applications of spectral methods, in: R. Voigt, D. Gottlieb, M.Y. Hussaini (Eds.), *Spectral Methods for Partial Differential Equations*, SIAM, Philadelphia, 1984, pp. 1–54.
- [10] D. Gottlieb, C.W. Shu, A. Solomonoff, H. Vandeven, On the Gibbs phenomenon I: recovering exponential accuracy from the Fourier partial sum of a non-periodic analytic function, *J. Comput. Appl. Math.* 43 (1992) 81–98.
- [11] D. Gottlieb, C.W. Shu, Resolution properties of the Fourier method for discontinuous waves, *Comput. Methods Appl. Mech. Engrg.* 116 (1994) 27–37.
- [12] D. Gottlieb, C.W. Shu, On the Gibbs phenomenon III: recovering exponential accuracy in a sub-interval from a spectral partial sum of a piecewise analytic function, *SIAM Numer. Anal.* 33 (1996) 280–290.
- [13] D. Gottlieb, C.W. Shu, On the Gibbs phenomenon IV: recovering exponential accuracy in a sub-interval from a Gegenbauer partial sum of a piecewise analytic function, *Math. Comput.* 64 (1995) 1081–1095.
- [14] D. Gottlieb, C.W. Shu, On the Gibbs phenomenon V: recovering exponential accuracy from collocation point values of a piecewise analytic function, *Numer. Math.* 71 (1995) 511–526.

- [15] L. Jameson, High order methods for resolving waves: number of points per wavelength, *SIAM J. Sci. Comput.* 15 (4) (2000) 417–439.
- [16] H.O. Kreiss, J. Oliger, Comparison of accurate methods for the integration of hyperbolic equations, *Tellus XXIV* (3) (1972).
- [17] E.E. Meshkov, Instability of the interface of two gases accelerated by a shock wave, *Izv. Akad. Nauk. SSSR Mekh. Zhidk. Gaza* 4 (1969) 101–104.
- [18] H. Padé, Mémoire sur les développements en fractions continues de la fonction exponentielle pouvant servir d'introduction à la théorie des fractions continues algébriques, *Ann. Fac. Sci. École Norm. Sup.* 16 (1899) 395–436.
- [19] C.W. Shu, S. Osher, Efficient implementation of essentially non-oscillatory shock-capturing schemes, II, *J. Comput. Phys.* 83 (1) (1989) 32–78.
- [20] D. Gottlieb, C.W. Shu, The Gibbs phenomenon and its resolution, *SIAM Rev.* 39 (1997) 644–668.
- [21] D. Gottlieb, C.W. Shu, General theory for the resolution of the Gibbs phenomenon, *Accademia Nazionale Dei Lincei, ATTI Dei Convegni Lincei* 147, 1998, pp. 39–48.
- [22] B.D. Shizgal, J.H. Jung, On the resolution of the Gibbs phenomenon, in press.
- [23] L. Emmel, S.M. Kaber, Y. Maday, Padé–Jacobi filtering for spectral approximations of discontinuous solutions, *Numerical Algorithms* (2002) in press.
- [24] T.A. Driscoll, B. Fornberg, Padé algorithm for the Gibbs phenomenon, *Numerical Algorithms* (2000) submitted for publication.
- [25] J.F. Geer, Rational trigonometric approximations using Fourier series partial sums, *J. Sci. Comput.* 10 (3) (1995) 325–356.
- [26] W.S. Don, O. Kaber, M.S. Min, in press.
- [27] S. Abarbanel, D. Gottlieb, E. Tadmor, Spectral methods for discontinuous problems, in: N.W. Morton, M.J. Baines (Eds.), *Numerical Methods for Fluid Dynamics II*, Oxford University Press, 1986, pp. 128–153.
- [28] P.D. Lax, Accuracy and resolution in the computation of solutions of linear and nonlinear equations, in: *Recent Advances in Numerical Analysis, Proc. Symp., Mathematical Research Center, University of Wisconsin*, Academic Press, 1978, pp. 107–117.
- [29] E. Tadmor, Convergence of spectral methods for nonlinear conservation laws, *SINUM* 26 (1989) 30–44.
- [30] E. Tadmor, Shock capturing by the spectral viscosity method, in: *Proceedings of ICOSAHOM 89*, Elsevier Science, North-Holland, IMACS, 1989.
- [31] Y. Maday, S. Ould Kaber, E. Tadmor, Legendre pseudospectral viscosity method for nonlinear conservation laws, *SIAM J. Numer. Anal.* 30 (1993) 321–342.
- [32] H. Ma, Chebyshev–Legendre super spectral viscosity method for nonlinear conservation laws, *SIAM J. Numer. Anal.*, submitted for publication.
- [33] M. Carpenter, D. Gottlieb, C.W. Shu, On the conservation and convergence to weak solutions of global schemes, *J. Sci. Comput.*, in press.
- [34] C.-W. Shu, P. Wong, A note on the accuracy of spectral method applied to nonlinear conservation laws, *J. Sci. Comput.* 10 (1995) 357–369.
- [35] S. Gottlieb, D. Gottlieb, C.W. Shu, in press.
- [36] D. Gottlieb, L. Lustman, S.A. Orszag, *SISC* 2 (1981) 296.
- [37] D. Gottlieb, L. Lustman, C.L. Streett, Spectral methods for two dimensional flows, in: *Spectral Methods for PDEs*, SIAM, Philadelphia, 1984.
- [38] W.S. Don, Numerical study of pseudospectral methods in shock wave applications, *J. Comput. Phys.* 110 (1994) 103–111.
- [39] W.S. Don, C. Quillen, Numerical simulation of reactive flow, Part I: resolution, *J. Comput. Phys.* 122 (1995) 244–265.
- [40] W.S. Don, D. Gottlieb, Spectral simulations of supersonic reactive flows, *SIAM J. Numer. Anal.* 35 (6) (1998) 2370–2384.